

On problematic case of product approximation in Backus average

Filip P. Adamus *

Abstract

Seismic anisotropy is often a combined effect of the intrinsic anisotropy and the anisotropy induced by thin-layering. The Backus average, a useful mathematical tool, allows us to describe the latter one quantitatively. The results are meaningful only if the underlying physical assumptions are obeyed, such as the low frequency of the propagating wave. In this paper, however, we focus on the only mathematical assumption of the Backus average, namely, product approximation. It states that the average of the product of a varying function with nearly-constant function is approximately equal to the product of the averages of those functions. We discuss particular, problematic case for which the aforementioned assumption is inaccurate. Further, we examine numerically if this inaccuracy affects the wave propagation in a homogenous medium—obtained using the Backus average—equivalent to thin layers. We take into consideration various material symmetries, including orthotropic, cubic, and others.

We show that the problematic case of product approximation is strictly related to the negative Poisson's ratio of constituent layers. Therefore, we discuss the laboratory and well-log cases in which such a ratio has been noticed. Upon thorough literature review, it occurs that examples of so-called auxetic rocks (rocks that have negative Poisson's ratio) are not extremely rare exceptions as thought previously. The investigation and derivation of Poisson's ratio for materials exhibiting symmetry classes up to monoclinic become a significant part of this paper.

Except for the main objectives of the paper, we additionally show that the averaging of cubic layers results in an equivalent medium having tetragonal (not cubic) symmetry. Also, we present concise formulations of stability conditions for low symmetry classes, such as trigonal, orthotropic, and monoclinic.

1 Introduction

The assumption of isotropy in media in which seismic wave propagates is convenient, but often inaccurate. Individual crystals composing a rock have to be neither of the same types nor oriented randomly. In case they are not, we encounter so-called intrinsic anisotropy. Further, due to geological processes, the formation of rocks can be arranged in a non-random manner forming a foliated structure. In such a situation, we consider anisotropy induced by thin layers.

The Backus average is a useful mathematical tool that provides us with a quantitative description of the anisotropy produced by thin layering (Backus, 1962). The isotropic layers can be replaced by the transversely-isotropic, equivalent (or, so-called, effective, or replacement) medium. The anisotropy of such medium is a consequence of the inhomogeneity of the stack of layers only (e.g., Slawinski, 2018, Chapter 4). Further, as also shown by Backus (1962), the transversely-isotropic constituents may be approximated by a transversely-isotropic medium, which anisotropy is a combined effect of the intrinsic anisotropy and the anisotropy induced by thin-layering (Bakulin and Grechka, 2003). The Backus average can be extended to lower symmetry classes. We can either follow the procedure analogous to

*Department of Earth Sciences, Memorial University of Newfoundland, Canada, adamusfp@gmail.com

the one shown by Backus (1962) or use the efficient matrix formalism presented by Schoenberg and Muir (1989).

The equivalent medium obtained using the Backus average is a good analogy of a layered material only if the underlying assumptions of the average are satisfied. In the literature, numerous authors dedicate their works to the assumption of thin layering and long wavelength of the signal. Among many of them are Helbig (1984), Carcione et al. (1991), or Liner and Fei (2007). Another, but mathematical assumption introduced by Backus (1962) is the one of product approximation, which states that the average of the product of a rapidly-varying function with nearly-constant function is approximately equal to the product of the averages of those functions. For more than a half-century, the researchers take the product assumption for granted. Bos et al. (2017) are the first authors to discuss its validity in the context of the Backus average. A year later, Bos et al. (2018) find and examine statistically a particular case for which the product approximation results in spurious values. They conclude that this problematic case is physically possible, but not likely to appear in seismology. The aforementioned authors examine a single example of a rapidly-varying function that corresponds to the isotropic layers only.

This paper aims to continue the investigation on the particular, problematic case of product approximation. However, we do not limit ourselves to the examples of rapidly-varying functions corresponding to isotropic layers, but we also check their analogous forms valid for anisotropic constituents. We discuss in detail the possibility of the occurrence of inaccurate product approximation in the context of seismology. We relate it to the presence of negative Poisson's ratio in individual thin layers. Rocks that exhibit such a ratio are called auxetic; in this work, we pay special attention to them. Finally, we perform several simulations of a wave propagating in thinly-layered and equivalent media. We compare the results to understand what is the practical influence of the problematic case of product assumption on the accuracy of the averaging process.

To be able to perform the investigation on product approximation and negative Poisson's ratio, first, we need to introduce the necessary tools and notions that we use later in the text. Therefore, in Section 2, we discuss symmetry classes of elasticity tensors, the conditions that must be obeyed to make these tensors stable, and details of the Backus average. Section 3 consists of the main body of the paper.

Can we, in any seismological scenarios, freely use the Backus average to approximate thinly layered material by the long-wave equivalent medium? The above question has to be posed and answered, hence this paper.

2 Theory

2.1 Symmetry classes of elasticity tensor

In the theory of linear elasticity, the forces applied to a single point are expressed in terms of a stress tensor and their resultant deformations in terms of a strain tensor. The definition of the strain tensor for infinitesimal displacements in three dimensions is

$$\varepsilon_{ij} := \frac{1}{2} \left(\frac{\partial u_i}{\partial x_j} + \frac{\partial u_j}{\partial x_i} \right) \quad i, j \in \{1, 2, 3\}, \quad (1)$$

where subscripts i and j , denote Cartesian coordinates, and u_i are the components of the displacement vector describing the deformations in the i -th direction. The constitutive equation relating stresses

and strains is Hooke's law, namely,

$$\sigma_{ij} = \sum_{k=1}^3 \sum_{\ell=1}^3 c_{ijkl} \varepsilon_{k\ell} \quad i, j \in \{1, 2, 3\}, \quad (2)$$

which states that the applied load at a point is linearly related to the deformation by the elasticity tensor, c_{ijkl} . We can replace c_{ijkl} by C_{mn} , where $m, n \in \{1, \dots, 6\}$, by following

$$\begin{cases} m = i & \text{if } i = j \\ n = \ell & \text{if } \ell = k \end{cases} \quad \text{and} \quad \begin{cases} m = 9 - (i + j) & \text{if } i \neq j \\ n = 9 - (\ell + k) & \text{if } \ell \neq k \end{cases}. \quad (3)$$

In this way, we can represent the elasticity tensor by 6×6 matrix. C_{mn} can be invariant to different groups of transformations of the coordinate system. The invariance to the orientation of the coordinate system is called material symmetry. There are eight possible symmetry classes. Herein, we focus on monoclinic, orthotropic, tetragonal, trigonal, transversely-isotropic (TI), cubic, and isotropic classes.

We call a tensor to be monoclinic if its symmetry group contains a reflection about a plane through the origin. Herein, for convenience, we choose x_3 to be the axis along which we perform the reflection. If we additionally rotate the coordinates about x_3 axis by angle θ , where $\tan(2\theta) = 2C_{45}/(C_{44} - C_{55})$, we can express the monoclinic tensor in its natural coordinate system (Helbig, 1994, p.83). In such an orientation, the elasticity matrix has the lowest possible number of the nonzero entries (Slawinski, 2015, Section 5.6.3). We obtain the following stress-strain relation expressed in a matrix form,

$$\begin{bmatrix} \sigma_{11} \\ \sigma_{22} \\ \sigma_{33} \\ \sigma_{23} \\ \sigma_{13} \\ \sigma_{12} \end{bmatrix} = \begin{bmatrix} C_{11} & C_{12} & C_{13} & 0 & 0 & C_{16} \\ C_{12} & C_{22} & C_{23} & 0 & 0 & C_{26} \\ C_{13} & C_{23} & C_{33} & 0 & 0 & C_{36} \\ 0 & 0 & 0 & C_{44} & 0 & 0 \\ 0 & 0 & 0 & 0 & C_{55} & 0 \\ C_{16} & C_{26} & C_{36} & 0 & 0 & C_{66} \end{bmatrix} \begin{bmatrix} \varepsilon_{11} \\ \varepsilon_{22} \\ \varepsilon_{33} \\ 2\varepsilon_{23} \\ 2\varepsilon_{13} \\ 2\varepsilon_{12} \end{bmatrix}. \quad (4)$$

The elasticity tensor whose symmetry group contains a two-fold, three-fold, four-fold, or n -fold rotation is called orthogonal, trigonal, tetragonal, or TI, respectively. Their matrix representations having the least nonzero independent entries are the following.

$$C^{\text{ort}} = \begin{bmatrix} C_{11} & C_{12} & C_{13} & 0 & 0 & 0 \\ C_{12} & C_{22} & C_{23} & 0 & 0 & 0 \\ C_{13} & C_{23} & C_{33} & 0 & 0 & 0 \\ 0 & 0 & 0 & C_{44} & 0 & 0 \\ 0 & 0 & 0 & 0 & C_{55} & 0 \\ 0 & 0 & 0 & 0 & 0 & C_{66} \end{bmatrix}, \quad C^{\text{trig}} = \begin{bmatrix} C_{11} & C_{12} & C_{13} & 0 & C_{15} & 0 \\ C_{12} & C_{11} & C_{13} & 0 & -C_{15} & 0 \\ C_{13} & C_{13} & C_{33} & 0 & 0 & 0 \\ 0 & 0 & 0 & C_{44} & 0 & -C_{15} \\ C_{15} & -C_{15} & 0 & 0 & C_{44} & 0 \\ 0 & 0 & 0 & -C_{15} & 0 & \frac{C_{11}-C_{12}}{2} \end{bmatrix}, \quad (5)$$

$$C^{\text{tetr}} = \begin{bmatrix} C_{11} & C_{12} & C_{13} & 0 & 0 & 0 \\ C_{12} & C_{11} & C_{13} & 0 & 0 & 0 \\ C_{13} & C_{13} & C_{33} & 0 & 0 & 0 \\ 0 & 0 & 0 & C_{44} & 0 & 0 \\ 0 & 0 & 0 & 0 & C_{44} & 0 \\ 0 & 0 & 0 & 0 & 0 & C_{66} \end{bmatrix}, \quad C^{\text{TI}} = \begin{bmatrix} C_{11} & C_{12} & C_{13} & 0 & 0 & 0 \\ C_{12} & C_{11} & C_{13} & 0 & 0 & 0 \\ C_{13} & C_{13} & C_{33} & 0 & 0 & 0 \\ 0 & 0 & 0 & C_{44} & 0 & 0 \\ 0 & 0 & 0 & 0 & C_{44} & 0 \\ 0 & 0 & 0 & 0 & 0 & \frac{C_{11}-C_{12}}{2} \end{bmatrix}. \quad (6)$$

Again, we choose the x_3 -axis to be the rotation axis. A cubic symmetry group contains four-fold rotations about two axes that are orthogonal to one another, whereas isotropic elasticity tensor is

invariant under any rotation. Their matrix representations are

$$C^{\text{cub}} = \begin{bmatrix} C_{11} & C_{13} & C_{13} & 0 & 0 & 0 \\ C_{13} & C_{11} & C_{13} & 0 & 0 & 0 \\ C_{13} & C_{13} & C_{11} & 0 & 0 & 0 \\ 0 & 0 & 0 & C_{44} & 0 & 0 \\ 0 & 0 & 0 & 0 & C_{44} & 0 \\ 0 & 0 & 0 & 0 & 0 & C_{44} \end{bmatrix} \quad (7)$$

and

$$C^{\text{iso}} = \begin{bmatrix} C_{11} & C_{11} - 2C_{44} & C_{11} - 2C_{44} & 0 & 0 & 0 \\ C_{11} - 2C_{44} & C_{11} & C_{11} - 2C_{44} & 0 & 0 & 0 \\ C_{11} - 2C_{44} & C_{11} - 2C_{44} & C_{11} & 0 & 0 & 0 \\ 0 & 0 & 0 & C_{44} & 0 & 0 \\ 0 & 0 & 0 & 0 & C_{44} & 0 \\ 0 & 0 & 0 & 0 & 0 & C_{44} \end{bmatrix}. \quad (8)$$

2.2 Stability conditions for various symmetries

The stability conditions constitute the fact that it is necessary to expand energy to deform a material. To satisfy these conditions, a 6×6 matrix that represents an elasticity tensor must be positive semidefinite. A real symmetric matrix is positive semidefinite if and only if all its eigenvalues (or, equivalently, its principal minors) are nonnegative. Any isotropic tensor is stable if

$$C_{11} \geq \frac{4}{3}C_{44} \geq 0. \quad (9)$$

A cubic tensor must satisfy

$$C_{11} - C_{13} \geq 0, \quad C_{11} + 2C_{13} \geq 0, \quad \text{and} \quad C_{44} \geq 0. \quad (10)$$

For a TI and tetragonal tensor we require

$$C_{11} - |C_{12}| \geq 0, \quad C_{33}(C_{11} + C_{12}) \geq 2C_{13}^2, \quad C_{44} \geq 0, \quad \text{and} \quad C_{66} \geq 0. \quad (11)$$

The last inequality is redundant for the TI case, due to relation $2C_{66} = C_{11} - C_{12}$. A trigonal tensor expressed in a natural coordinate system is stable if

$$C_{11} - |C_{12}| \geq 0, \quad C_{33}(C_{11} + C_{12}) \geq 2C_{13}^2, \quad C_{44} \geq 0, \quad \text{and} \quad C_{11} - C_{12} \geq 2\frac{C_{15}^2}{C_{44}}. \quad (12)$$

These inequalities are more complicated if a trigonal tensor is not expressed with respect to its natural coordinate system. In such a case, not analyzed herein, $C_{14} \neq 0$. So far we have obtained the above stability conditions by verifying the requirements for nonnegative eigenvalues. In the case of orthotropic and monoclinic symmetry classes, due to complicated forms of eigenvalues, we follow the nonnegative, principal-minors criterium. For the orthotropic tensor, we get

$$C_{11} \geq 0, \quad C_{11}C_{22} \geq C_{12}^2, \quad C_{44} \geq 0, \quad C_{55} \geq 0, \quad C_{66} \geq 0, \quad \text{and} \quad (13)$$

$$C_{11}C_{22}C_{33} + 2C_{12}C_{13}C_{23} - C_{11}C_{23}^2 - C_{22}C_{13}^2 - C_{33}C_{12}^2 \geq 0. \quad (14)$$

A monoclinic tensor is stable if inequalities (13), (14), and

$$\begin{aligned} & C_{11}C_{22}C_{33} + 2C_{12}C_{13}C_{23} - C_{11}C_{23}^2 - C_{22}C_{13}^2 - C_{33}C_{12}^2 \geq \\ & C_{16}^2(C_{22}C_{33} - C_{23}^2) + C_{26}^2(C_{11}C_{33} - C_{13}^2) + C_{36}^2(C_{11}C_{22} - C_{12}^2) + \\ & 2C_{16}C_{26}(C_{13}C_{23} - C_{33}C_{12}) + 2C_{16}C_{36}(C_{12}C_{23} - C_{22}C_{13}) + 2C_{26}C_{36}(C_{12}C_{13} - C_{11}C_{23}) \end{aligned} \quad (15)$$

are satisfied. The inequalities are even more complicated for a non-natural coordinate system, where $C_{45} \neq 0$. We notice that for any symmetry class all the main-diagonal entries of the elasticity matrix must be nonnegative, which is simple to prove (e.g. Slawinski, 2015, Exercise 4.5). Notice that the stability conditions for some of the symmetry classes are discussed in Mouchat and Coudert (2014).

2.3 Backus average

The procedure of Backus averaging is based on the assumption that the averaged medium is in static equilibrium. If the top and bottom of such a medium is subjected to the same stresses, and we set the Cartesian coordinate system in such a manner that the x_3 -axis is vertical, then

$$\sigma_{i3}, \quad \frac{\partial u_i}{\partial x_2}, \quad \frac{\partial u_i}{\partial x_1}, \quad i \in \{1, 2, 3\} \quad (16)$$

are vertically constant. The remaining stresses or strains may vary significantly along x_3 -axis.

Physically, the above assumption is satisfied, and the Backus average makes sense, if the thickness of the averaged stack of layers, l' , is much smaller than the wavelength. In other words, the lower wave frequency, the better accuracy of the average. For purposes of our numerical tests, performed in Section 3.3, we choose l' to be at least ten times shorter than the dominant wavelength of primary wave, λ_0^P , which assures that the long-wave assumption is satisfied (Carcione et al., 1991).

Mathematically, the Backus average is correct if the only one mathematical assumption introduced by Backus, namely, the product approximation, remains true. As Backus states in his paper,

$$\overline{f(x_3)g(x_3)} \approx \overline{f(x_3)} \overline{g(x_3)}, \quad (17)$$

where, overbar denotes the average weighted by the layer thicknesses. $f(x_3)$ is a nearly-constant function that stands for stresses and displacements from expression (16). $g(x_3)$ describes combinations of elasticity parameters, which can vary significantly from layer to layer. If the above approximation holds, the elasticity coefficients of a stack of isotropic layers are long-wave equivalent to

$$\begin{aligned} C_{11}^{\overline{\text{TI}}} &= \overline{\left(\frac{C_{11} - 2C_{44}}{C_{11}}\right)^2} \overline{\left(\frac{1}{C_{11}}\right)}^{-1} + \overline{\left(\frac{4(C_{11} - C_{44})C_{44}}{C_{11}}\right)}, \\ C_{13}^{\overline{\text{TI}}} &= \overline{\left(\frac{C_{11} - 2C_{44}}{C_{11}}\right)} \overline{\left(\frac{1}{C_{11}}\right)}^{-1}, \\ C_{33}^{\overline{\text{TI}}} &= \overline{\left(\frac{1}{C_{11}}\right)}^{-1}, \\ C_{44}^{\overline{\text{TI}}} &= \overline{\left(\frac{1}{C_{44}}\right)}^{-1}, \\ C_{66}^{\overline{\text{TI}}} &= \overline{C_{44}}, \end{aligned} \quad (18)$$

where C_{11} and C_{44} describe each isotropic layer. The five independent coefficients on the left-hand side are the equivalent transversely-isotropic parameters. In Appendix A, we present formulation of the Backus average for layers that exhibit lower symmetry classes.

3 Problematic case of product approximation

As discussed by Bos et al. (2018), the assumption of product approximation may be inaccurate only in the case of $\bar{g} \approx 0$. Since, in such a situation, the relative error,

$$err = \frac{\overline{fg} - \bar{f}\bar{g}}{\bar{f}\bar{g}} \times 100\%, \quad (19)$$

is around 100%. Predominantly, g is positive (Bos et al., 2018). Therefore, in this section, we look for the possibilities of negative, or low positive g 's in layers so that the averaged medium have a chance to represent the problematic case of $\bar{g} \approx 0$. First, in Section 3.1, we study the problem from the theoretical point of view. We analyze various examples of functions g that describe combinations of elasticity coefficients corresponding to different symmetry classes. Subsequently, in Section 3.2, we look into the close relationship between Poisson's ratio and g . Based on this relation, we discuss the possibility of occurrence of $\bar{g} \approx 0$ in the real seismological cases. Lastly, in Section 3.3, we choose theoretically and practically possible values of elasticity parameters for each layer, such that the resulting $\bar{g} \approx 0$. Based on numerical experiments, we compare the simulation of a wave propagating in the layered and long-wave equivalent medium.

3.1 Negative g

Let us examine to which combinations of elasticity parameters function g corresponds. Herein, we consider symmetry classes up to monoclinic. To derive g , as an example, we perform the standard procedure to get Backus average for the monoclinic symmetry. First, we write the stress-strain relations in such medium as

$$\sigma_{11} = C_{11}\varepsilon_{11} + C_{12}\varepsilon_{22} + C_{13}\varepsilon_{33} + 2C_{16}\varepsilon_{12}, \quad (20)$$

$$\sigma_{22} = C_{12}\varepsilon_{11} + C_{22}\varepsilon_{22} + C_{23}\varepsilon_{33} + 2C_{26}\varepsilon_{12}, \quad (21)$$

$$\sigma_{33} = C_{13}\varepsilon_{11} + C_{23}\varepsilon_{22} + C_{33}\varepsilon_{33} + 2C_{36}\varepsilon_{12}, \quad (22)$$

$$\sigma_{23} = C_{44}\frac{\partial u_2}{\partial x_3} + C_{44}\frac{\partial u_3}{\partial x_2}, \quad (23)$$

$$\sigma_{13} = C_{55}\frac{\partial u_1}{\partial x_3} + C_{55}\frac{\partial u_3}{\partial x_1}, \quad (24)$$

$$\sigma_{12} = C_{16}\varepsilon_{11} + C_{26}\varepsilon_{22} + C_{36}\varepsilon_{33} + 2C_{66}\varepsilon_{12}. \quad (25)$$

Then, we rewrite the above equations. We want to have one component of a stress tensor or displacement vector that may vary along x_3 axis on one side of the equations, whereas on the other side the components that are nearly constant. We can directly do it with equations (22)–(24), namely,

$$\varepsilon_{33} = \sigma_{33} \underbrace{\left(\frac{1}{C_{33}}\right)}_{g_1} - \underbrace{\left(\frac{C_{13}}{C_{33}}\right)}_{g_2} \varepsilon_{11} - \underbrace{\left(\frac{C_{23}}{C_{33}}\right)}_{g_3} \varepsilon_{22} - \underbrace{\left(\frac{C_{36}}{C_{33}}\right)}_{g_{m_1}} 2\varepsilon_{12}, \quad (26)$$

$$\frac{\partial u_2}{\partial x_3} = \sigma_{23} \underbrace{\left(\frac{1}{C_{44}}\right)}_{g_4} - \frac{\partial u_3}{\partial x_2}, \quad (27)$$

$$\frac{\partial u_1}{\partial x_3} = \sigma_{13} \underbrace{\left(\frac{1}{C_{55}} \right)}_{g_5} - \frac{\partial u_3}{\partial x_1}. \quad (28)$$

Now, we insert the right-hand side of equation (26) into equations (20), (21), and (25), so we get,

$$\sigma_{11} = \sigma_{33} \left(\frac{C_{13}}{C_{33}} \right) + \underbrace{\left(C_{11} - \frac{C_{13}^2}{C_{33}} \right)}_{g_6} \varepsilon_{11} + \underbrace{\left(C_{12} - \frac{C_{13}C_{23}}{C_{33}} \right)}_{g_7} \varepsilon_{22} + \underbrace{\left(C_{16} - \frac{C_{13}C_{36}}{C_{33}} \right)}_{g_{m_2}} 2\varepsilon_{12}, \quad (29)$$

$$\sigma_{22} = \sigma_{33} \left(\frac{C_{23}}{C_{33}} \right) + \left(C_{12} - \frac{C_{13}C_{23}}{C_{33}} \right) \varepsilon_{11} + \underbrace{\left(C_{22} - \frac{C_{23}^2}{C_{33}} \right)}_{g_8} \varepsilon_{22} + \underbrace{\left(C_{26} - \frac{C_{23}C_{36}}{C_{33}} \right)}_{g_{m_3}} 2\varepsilon_{12}, \quad (30)$$

$$\sigma_{12} = \sigma_{33} \left(\frac{C_{36}}{C_{33}} \right) + \left(C_{16} - \frac{C_{13}C_{36}}{C_{33}} \right) \varepsilon_{11} + \left(C_{26} - \frac{C_{23}C_{36}}{C_{33}} \right) \varepsilon_{22} + \underbrace{\left(C_{66} - \frac{C_{36}^2}{C_{33}} \right)}_{g_9} 2\varepsilon_{12}. \quad (31)$$

Equations (26)–(31) are ready to be averaged. However, to be able to proceed with the Backus average, from now on, we need to introduce the assumption of product approximation (see Appendix A). Terms in parenthesis in equations (26)–(31) correspond to various g ; we denote them as g_i or g_{m_i} . Terms outside of parenthesis correspond to slowly varying function f . Expressions g_i are also presented in higher symmetry classes, and if we follow the procedure shown above, they occupy the analogical places as in equations (26)–(31). On the other hand, g_{m_i} , are typical for a monoclinic symmetry class only; they do not have the analogical terms in higher symmetry classes. As shown in Appendix B, in trigonal symmetry there is a special case of g that also does not find the analogy in other symmetries. We denote it by g_t . In Table 1, we indicate all possibilities of g 's for seven symmetry classes.

Based on stability conditions and analysis performed below, in Table 2, we present for which g 's the negative values are allowed. As can be easily verified numerically, the stability conditions allow C_{13} and C_{23} to be negative, thus, g_2 and g_3 are not necessarily positive. Since it is required that $C_{ii} \geq 0$ (for $i \in \{1, \dots, 6\}$), we conclude that all g_1 , g_4 , g_5 , and particular g_9 must be nonnegative. Below, we analyze only the cases in which it is non-trivial to decide if g 's are allowed to be negative. Since, the verdicts of possible negativity of g 's are obvious in cases of isotropic and cubic symmetries, let us discuss g_6 and g_7 for TI and tetragonal symmetries. We invoke condition

$$C_{33}(C_{11} + C_{12}) \geq 2C_{13}^2. \quad (32)$$

We know also that $C_{11} > C_{12}$. From the both conditions we obtain

$$C_{33}C_{11} \geq C_{13}^2, \quad (33)$$

and we infer that

$$C_{33}C_{12} \geq C_{13}^2 \quad (34)$$

is not necessarily true, hence, g_7^{TI} and g_7^{tetr} may be negative, whereas g_6^{TI} and g_6^{tetr} are always non-negative. For trigonal symmetry, the situation is more complicated, due to parameter C_{15} . g_9^{trig} is always nonnegative, due to condition

$$\frac{(C_{11} - C_{12})}{2} \geq \frac{C_{15}^2}{C_{44}}. \quad (35)$$

	monoclinic (g^{mon})	orthotropic (g^{ort})	trigonal (g^{trig})	tetragonal (g^{tetr})
g_1	$1/C_{33}$	$1/C_{33}$	$1/C_{33}$	$1/C_{33}$
g_2	C_{13}/C_{33}	C_{13}/C_{33}	C_{13}/C_{33}	C_{13}/C_{33}
g_3	C_{23}/C_{33}	C_{23}/C_{33}	g_2^{trig}	g_2^{tetr}
g_4	$1/C_{44}$	$1/C_{44}$	$1/C_{44}$	$1/C_{44}$
g_5	$1/C_{55}$	$1/C_{55}$	g_4^{trig}	g_4^{tetr}
g_6	$C_{11} - C_{13}^2/C_{33}$	$C_{11} - C_{13}^2/C_{33}$	$C_{11} - C_{13}^2/C_{33} - C_{15}^2/C_{44}$	$C_{11} - C_{13}^2/C_{33}$
g_7	$C_{12} - C_{13}C_{23}/C_{33}$	$C_{12} - C_{13}C_{23}/C_{33}$	$C_{12} - C_{13}^2/C_{33} + C_{15}^2/C_{44}$	$C_{12} - C_{13}^2/C_{33}$
g_8	$C_{22} - C_{23}^2/C_{33}$	$C_{22} - C_{23}^2/C_{33}$	g_6^{trig}	g_6^{tetr}
g_9	$C_{66} - C_{36}^2/C_{33}$	C_{66}	$(C_{11} - C_{12})/2 - C_{15}^2/C_{44}$	C_{66}
g_{m_1}	C_{36}/C_{33}			
g_{m_2}	$C_{16} - C_{13}C_{36}/C_{33}$			
g_{m_3}	$C_{26} - C_{23}C_{36}/C_{33}$			
g_t			C_{15}/C_{44}	
	TI (g^{TI})	cubic (g^{cub})	isotropic (g^{iso})	
g_1	$1/C_{33}$	$1/C_{11}$	$1/C_{11}$	
$g_2 = g_3$	C_{13}/C_{33}	C_{13}/C_{11}	$(C_{11} - 2C_{44})/C_{11}$	
$g_4 = g_5$	$1/C_{44}$	$1/C_{44}$	$1/C_{44}$	
$g_6 = g_8$	$C_{11} - C_{13}^2/C_{33}$	$C_{11} - C_{13}^2/C_{11}$	$4(C_{11} - C_{44})C_{44}/C_{11}$	
g_7	$C_{12} - C_{13}^2/C_{33}$	$C_{13} - C_{13}^2/C_{11}$	$2(C_{11} - 2C_{44})C_{44}/C_{11}$	
g_9	$(C_{11} - C_{12})/2$	C_{44}	C_{44}	

Table 1: Specific g 's for symmetry classes up to monoclinic.

monoclinic	orthotropic	trigonal	tetragonal	TI	cubic	isotropic
g_2^{mon}	g_2^{ort}	g_2^{trig}	g_2^{tetr}	g_2^{TI}	g_2^{cub}	g_2^{iso}
g_3^{mon}	g_3^{ort}	g_7^{trig}	g_7^{tetr}	g_7^{TI}		g_7^{iso}
g_7^{mon}	g_7^{ort}	g_t				
g_{m_1}						
g_{m_2}						
g_{m_3}						

Table 2: Possibly negative g 's for symmetry classes up to monoclinic.

Now we can analyze g_6^{trig} . We know that $C_{11} - C_{13}^2/C_{33}$ is nonnegative. To make it negative we try to subtract something greater or equal than C_{15}^2/C_{44} , which is $(C_{11} - C_{12})/2$. We obtain

$$C_{11} - \frac{C_{13}^2}{C_{33}} - \frac{C_{11} - C_{12}}{2} = \frac{\frac{1}{2}C_{33}(C_{11} + C_{12})}{C_{33}} - \frac{C_{13}^2}{C_{33}} \geq 0. \quad (36)$$

Thus, g_6^{trig} must be nonnegative. If $C_{15} = 0$ then $g_7^{\text{trig}} = g_7^{\text{tetr}} = g_7^{\text{TI}}$ and it means that g_7^{trig} can be negative the same as g_7^{tetr} and g_7^{TI} can. The additional stability condition (35) for trigonal symmetry—its other conditions are the same for TI and tetragonal symmetry—does allow it. Also, we numerically check that C_{15}/C_{44} can be negative; thus, g_t may be negative as well.

Let us discuss the orthotropic and monoclinic case. Due to the complexity of inequalities (14) and (15), to decide whether particular g are allowed to be negative, we perform numerical—instead of analytical—analysis only. Based on Monte Carlo (MC) simulations, we notice that g_7^{ort} , g_7^{mon} , g_{m_1} , g_{m_2} , or g_{m_3} can be negative while the eigenvalues of the tensors are still positive. We neither have found an orthotropic matrix with six nonnegative eigenvalues, where $g_6^{\text{ort}} < 0$ or $g_8^{\text{ort}} < 0$, nor monoclinic, semipositive matrix, where $g_6^{\text{mon}} < 0$, $g_8^{\text{mon}} < 0$, or $g_9^{\text{mon}} < 0$. Thus, we conclude that the above g 's must be nonnegative and we do not include them in Table 2.

3.2 Negative Poisson's ratio

3.2.1 Relation between g and Poisson's ratio

In this section, we look for the alternative elastic moduli that may indicate negative g . Especially, we focus on the relationship between $g < 0$ and negative Poisson's ratio. First, let us discuss the isotropic symmetry class. To have more physical insight in possibly negative g_2^{iso} and g_7^{iso} , we can express it in terms of Lamé parameters or bulk modulus and rigidity. Knowing that $\lambda := C_{11} - 2C_{44}$ and $\mu := C_{44}$, we rewrite

$$g_2^{\text{iso}} = \frac{\lambda}{\lambda + 2\mu} = \frac{K - \frac{2}{3}\mu}{K + \frac{4}{3}\mu} \quad \text{and} \quad g_7^{\text{iso}} = \frac{2\lambda\mu}{\lambda + 2\mu} = \frac{2(K - \frac{2}{3}\mu)\mu}{K + \frac{4}{3}\mu}, \quad (37)$$

where $K := \lambda + (2/3)\mu$ denotes pure compressibility and μ stands for sole rigidity. The material is stable if $\lambda \geq -(2/3)\mu$, $\mu \geq 0$, and $K \geq 0$. Thus, the denominators of expression (37) must be positive. Therefore, g_2^{iso} and g_7^{iso} are negative if and only if

$$\lambda < 0 \quad \text{or} \quad \frac{\text{compressibility}}{\text{rigidity}} := \frac{K}{\mu} < \frac{2}{3}. \quad (38)$$

The magnitudes of g_2^{iso} and g_7^{iso} are incomparable, since g_2^{iso} is dimensionless, whereas g_7^{iso} is not. We can express the Poisson's ratio, ν , in terms of Lamé parameters, or primary and secondary waves, namely,

$$\nu_{31} := -\frac{\varepsilon_{11}}{\varepsilon_{33}} = \frac{\lambda}{2(\lambda + \mu)} = \frac{V_P^2 - 2V_S^2}{2(V_P^2 - V_S^2)} = \nu_{ij} \quad i, j \in \{1, 2, 3\}. \quad (39)$$

The above expression is derived for uniaxial stress in the x_3 direction, but is valid for any direction. We denote the axial strain by letter i , while j stands for the lateral strain. Poisson's ratio is stable if the denominator $2(\lambda + \mu)$ is positive. Hence, negative numerator, λ , implies negative ν . Therefore, negative Poisson's ratio is another indicator of negative g_2^{iso} and g_7^{iso} . Also, notice that $\nu < 0$ if $V_P/V_S < \sqrt{2}$. Let us discuss, the cubic symmetry. In such a case, g is negative if and only if C_{13} is negative, which is tantamount to negative Poisson's ratio, since we have

$$\nu_{ij} = \frac{C_{13}}{C_{11} + C_{13}} \quad (40)$$

and to satisfy the stability condition the denominator must be positive. For TI and tetragonal symmetries, Poisson's ratio

$$\nu_{31} = \nu_{32} = \frac{C_{13}}{C_{11} + C_{12}}, \quad \nu_{13} = \nu_{23} = \frac{C_{13}(C_{11} - C_{12})}{C_{33}C_{11} - C_{13}^2} \quad (41)$$

is negative if and only if g_2 is negative (C_{13} must be less than zero) and

$$\nu_{21} = \nu_{12} = \frac{C_{33}C_{12} - C_{13}^2}{C_{33}C_{11} - C_{13}^2} \quad (42)$$

is negative if and only if g_7 is negative. Note that expressions (39), (41), and (42) are also derived in Mavko et al. (2009). For the trigonal symmetry class, we get the following Poisson's ratios.

$$\nu_{31} = \nu_{32} = \frac{C_{13} \left(C_{11} - C_{12} - 2 \frac{C_{15}^2}{C_{44}} \right)}{C_{11} \left(C_{11} - 2 \frac{C_{15}^2}{C_{44}} \right) - C_{12} \left(C_{12} + 2 \frac{C_{15}^2}{C_{44}} \right)}, \quad (43)$$

$$\nu_{21} = \nu_{12} = \frac{C_{12} - \frac{C_{13}^2}{C_{33}} + \frac{C_{15}^2}{C_{44}}}{C_{11} - \frac{C_{13}^2}{C_{33}} - \frac{C_{15}^2}{C_{44}}} = \frac{g_7^{\text{trig}}}{g_6^{\text{trig}}}, \quad (44)$$

$$\nu_{13} = \nu_{23} = \frac{\frac{C_{13}}{C_{33}} \left(C_{11} - C_{12} - 2 \frac{C_{15}^2}{C_{44}} \right)}{C_{11} - \frac{C_{13}^2}{C_{33}} - \frac{C_{15}^2}{C_{44}}} = \frac{g_2^{\text{trig}} a}{g_6^{\text{trig}}}. \quad (45)$$

Let us discuss expression (43). The term in the nominator in parenthesis, to which we later refer as a , must be nonnegative due to the last inequality in condition (12). Thus, first parenthesis in the denominator must be also positive and equal or larger than C_{12} . Second parenthesis must be equal or smaller than C_{11} . Therefore, the denominator must be positive. Due to the above analysis, we notice that ν_{31} and ν_{32} are negative if and only if C_{13} is negative. In other words, negative g_2^{trig} is tantamount to negative ν_{31} or ν_{32} . On the other hand, according to expression (44), negative g_7^{trig} is tantamount to negative ν_{21} . Lastly, ν_{13} and ν_{23} are negative if and only if $g_2^{\text{trig}} < 0$. For orthotropic symmetry class we get

$$\nu_{31} = \frac{C_{13}C_{22} - C_{12}C_{23}}{C_{11}C_{22} - C_{12}^2} = \frac{n_1}{d_3}, \quad (46)$$

$$\nu_{32} = \frac{C_{23}C_{11} - C_{12}C_{13}}{C_{11}C_{22} - C_{12}^2} = \frac{n_2}{d_3}, \quad (47)$$

$$\nu_{21} = \frac{C_{12}C_{33} - C_{13}C_{23}}{C_{11}C_{33} - C_{13}^2} = \frac{n_3}{d_2}, \quad (48)$$

$$\nu_{23} = \frac{C_{23}C_{11} - C_{12}C_{13}}{C_{11}C_{33} - C_{13}^2} = \frac{n_2}{d_2}, \quad (49)$$

$$\nu_{12} = \frac{C_{12}C_{33} - C_{13}C_{23}}{C_{22}C_{33} - C_{23}^2} = \frac{n_3}{d_1}, \quad (50)$$

$$\nu_{13} = \frac{C_{13}C_{22} - C_{12}C_{23}}{C_{22}C_{33} - C_{23}^2} = \frac{n_1}{d_1}, \quad (51)$$

where denominators d_1 , d_2 , and d_3 must be positive due to the stability conditions. Numerator $n_3 = C_{33} g_7^{\text{ort}}$, hence, negative g_7^{ort} implies negative ν_{21} and ν_{12} . The analysis of numerators n_1 and n_2 is more complicated since we cannot simply express it in terms of g_i^{ort} . However, based on MC simulations we notice that:

- if $g_2^{\text{ort}} < 0$ and $g_3^{\text{ort}} < 0$ then n_1 and n_2 cannot be both positive,
- if $g_2^{\text{ort}} > 0$ and $g_3^{\text{ort}} > 0$ then n_1 and n_2 cannot be both negative,
- if $g_2^{\text{ort}} > 0$ and $g_3^{\text{ort}} < 0$ then both $n_1 < 0$ and $n_2 > 0$ are not allowed,
- if $g_2^{\text{ort}} < 0$ and $g_3^{\text{ort}} > 0$ then both $n_1 > 0$ and $n_2 < 0$ are not allowed.

The above statements are proved analytically in Appendix C.

For a monoclinic symmetry we get

$$\nu_{31} = \frac{C_{13}C_{26}^2 - C_{16}C_{23}C_{26} - C_{12}C_{26}C_{36} + C_{16}C_{22}C_{36} + C_{12}C_{23}C_{66} - C_{13}C_{22}C_{66}}{C_{66}C_{12}^2 - 2C_{12}C_{16}C_{26} + C_{22}C_{16}^2 + C_{11}C_{26}^2 - C_{11}C_{22}C_{66}} = \frac{n_1}{d_3}, \quad (52)$$

$$\nu_{32} = \frac{C_{16}^2C_{23} - C_{13}C_{16}C_{26} - C_{12}C_{16}C_{36} + C_{11}C_{26}C_{36} + C_{12}C_{13}C_{66} - C_{11}C_{23}C_{66}}{C_{66}C_{12}^2 - 2C_{12}C_{16}C_{26} + C_{22}C_{16}^2 + C_{11}C_{26}^2 - C_{11}C_{22}C_{66}} = \frac{n_2}{d_3}, \quad (53)$$

$$\nu_{21} = \frac{C_{12}C_{36}^2 - C_{13}C_{26}C_{36} - C_{16}C_{23}C_{36} + C_{16}C_{26}C_{33} + C_{13}C_{23}C_{66} - C_{12}C_{33}C_{66}}{C_{66}C_{13}^2 - 2C_{13}C_{16}C_{36} + C_{33}C_{16}^2 + C_{11}C_{36}^2 - C_{11}C_{33}C_{66}} = \frac{n_3}{d_2}, \quad (54)$$

$$\nu_{23} = \frac{C_{16}^2C_{23} - C_{13}C_{16}C_{26} - C_{12}C_{16}C_{36} + C_{11}C_{26}C_{36} + C_{12}C_{13}C_{66} - C_{11}C_{23}C_{66}}{C_{66}C_{13}^2 - 2C_{13}C_{16}C_{36} + C_{33}C_{16}^2 + C_{11}C_{36}^2 - C_{11}C_{33}C_{66}} = \frac{n_2}{d_2}, \quad (55)$$

$$\nu_{12} = \frac{C_{12}C_{36}^2 - C_{13}C_{26}C_{36} - C_{16}C_{23}C_{36} + C_{16}C_{26}C_{33} + C_{13}C_{23}C_{66} - C_{12}C_{33}C_{66}}{C_{66}C_{23}^2 - 2C_{23}C_{26}C_{36} + C_{33}C_{26}^2 + C_{22}C_{36}^2 - C_{22}C_{33}C_{66}} = \frac{n_3}{d_1}, \quad (56)$$

$$\nu_{13} = \frac{C_{13}C_{26}^2 - C_{16}C_{23}C_{26} - C_{12}C_{26}C_{36} + C_{16}C_{22}C_{36} + C_{12}C_{23}C_{66} - C_{13}C_{22}C_{66}}{C_{66}C_{23}^2 - 2C_{23}C_{26}C_{36} + C_{33}C_{26}^2 + C_{22}C_{36}^2 - C_{22}C_{33}C_{66}} = \frac{n_1}{d_1}. \quad (57)$$

Due to complicated forms of Poisson's ratios, we again are not able to analytically express the relationship between the sign of ν and its influence on g . Based on MC simulations, we notice that the negative sign of alone g_2^{mon} , g_3^{mon} , g_7^{mon} , g_{m_1} , g_{m_2} , or alone g_{m_3} cannot restrict the sign of any ν_{ij} . Also, all negative or all positive Poisson's ratios do not imply the negative sign of any g . There are, however, some combinations of negative g that imply negative sign of certain ν_{ij} . For instance, negative g_2^{mon} , g_3^{mon} , and g_7^{mon} , or negative g_7^{mon} , g_{m_2} , and g_{m_3} , or negative g_3^{mon} , g_{m_1} , and g_{m_3} , imply that certain ν_{ij} must be negative.

To conclude, for isotropic, cubic, TI, and tetragonal symmetries, negative Poisson's ratio in any axial direction implies some negative g , and any negative g implies some $\nu_{ij} < 0$. The above is not always true for trigonal and orthotropic symmetries. In case of a trigonal symmetry class, negative g_t , and in case of an orthotropic class, negative g_2^{ort} or negative g_3^{ort} , do not imply that certain $\nu_{ij} < 0$. In monoclinic case, negative ν (in all axial directions) does not imply negative sign of any g , but some combinations of negative g 's imply that certain $\nu_{ij} < 0$.

3.2.2 Crystals, minerals and rocks with negative Poisson's ratio

Since, in the majority of symmetry classes examined by us, the presence of negative Poisson's ratio is tantamount to some negative g , it is reasonable to check the sign of this ratio for the layered rocks. The appearance of $g < 0$ in some individual layers may lead to $\bar{g} \approx 0$ of the equivalent medium that, in turn, can cause the inaccuracy of Backus approximation. In general, $\nu < 0$ is not likely to occur in geophysical data, however, as Zaitsev et al. (2017) state,

rocks with negative Poisson ratios are not rare exceptions, in contrast to conventional belief.

As numerically shown by Kudela and Stanoev (2018), negative Poisson's ratio does not occur in the global seismological case exemplified by the Preliminary reference Earth model (Dziewoński and

Anderson, 1981). However, there are some laboratory and well-log cases in which $\nu < 0$ has been noticed locally. By doing a detailed literature review, we invoke them below.

First, let us discuss naturally occurring auxetic crystals and minerals that have been investigated in a laboratory. Using spectroscopic techniques, Yeganeh-Haeri et al. (1992) show that α -cristobalite, which is a low-temperature modification of a crystalline form of silica (SiO_2), exhibit negative Poisson's ratio. Due to its elastic anisotropy, the value of ν varies with the direction of uniaxial stress. Poisson's ratio occurs to range from -0.5 to 0.08 , although it remains predominantly negative. Cristobalite widely occurs in nature (Yeganeh-Haeri et al., 1992). It forms in volcanic lava domes and often can be found in acidic volcanic rocks (Damby et al., 2014). Also, it can occur in soils (Mizota et al., 1987), deep-sea cherts and porcelanites (Calvert et al., 1977), or other sedimentary rocks (Beljankin and Petrov, 1938). Therefore, one should not disregard its potential influence on the rock's Poisson's ratio. A mineral that also may have $\nu < 0$ is zeolite (Grima et al. (2000), Grima et al. (2007), Sanchez-Valle et al. (2008)). It naturally occurs, for instance, in deep-sea sediments or geothermal systems (Hay, 1986). More, however, very rare auxetic minerals are indicated by Baughman et al. (1998). Also, as stated by Lakes (2017), it is more likely for the highly anisotropic minerals or crystals to have negative Poisson's ratio, than for the isotropic ones. For instance, single-crystal form of anisotropic arsenic, antimony, and bismuth exhibit $\nu < 0$ in certain directions. However, there is a case of an auxetic mineral that is isotropic. It occurs that, depending on the temperature, polycrystalline quartz exhibits low, very low, or negative Poisson's ratio (McKnight et al., 2008). According to Ji et al. (2010), the presence of this mineral may render some rocks to be auxetic. At ambient conditions, the Poisson's ratio of quartz is $\nu = 0.08$ (Ji et al., 2018).

Let us invoke some laboratory examples of various auxetic rocks. Nur and Simmons (1969) have noticed that very small or negative values of ν are exhibited by dry rocks at very low pressure. They observed that, if there is no external pressure, Casco and Westerly granites present $\nu = -0.100$ and $\nu = -0.094$, respectively. Twenty years later, Hommand-Etienne and Houpert (1989) examine Senones and Remiremont granites with thermally induced cracks. These rocks occur to have negative Poisson's ratio for various directions of uniaxial stresses, which is probably caused, as authors state, by numerous microcracks. The investigation of Zaitsev et al. (2017) confirm that negative ν can primarily occur in cracked rocks at low pressures. Based on the works of Coyner (1984), Freund (1992), and Mavko and Jizba (1994), they invoke 34 rock samples of cracked rocks with $\nu < 0$ at 8MPa confining pressure. Gregory (1976) examined 20 samples of sedimentary rocks at different pressures and at ambient temperature. He notices that apart from the low pressure, $\nu < 0$ (presented in many examined samples) is caused by gas saturation and low porosity. The above statement is confirmed by the experiments of Han (1986) and Jizba (1991). In their works, negative Poisson's ratio is exhibited only by low-porous sedimentary rocks; consolidated sandstones and gas sandstones, respectively. Such results were obtained, *inter alia*, for the approximate effective pressure in the well, that is, for 20MPa (Dvorkin et al., 1999). Ji et al. (2010) show that ν decreases with increasing temperature due to thermal effects. According to the authors, quartz-rich rocks at a temperature approaching the α - β quartz transition (such as granite, diorite, quartz-rich sandstone, etc.) may display negative values of Poisson's ratio. They use quartzite as an example to illustrate the effect of phase transition on ν . The quartz-transition temperature is at about 600°C , however, quartzite has $\nu = 0$ at the temperature of 450°C only. Between 450°C and 600°C it exhibits $\nu < 0$ (Ji et al., 2010, Figure 3b). Recently, the topic of auxetic natural rocks has been studied carefully by Ji et al. (2018). They state that

none of the crystalline igneous and metamorphic rocks (e.g., amphibolite, gabbro, granite, peridotite, and schist) display auxetic behavior at pressures of > 5 MPa and room temperature. Our experimental measurements showed that quartz-rich sedimentary rocks (i.e., sandstone and siltstone) are most likely to be the only rocks with negative Poisson's ratios at low confining pressures (≤ 200 MPa) because their main constituent mineral, α -quartz, already has extremely low Poisson's ratio ($\nu = 0.08$) and they contain microcracks,

micropores, and secondary minerals.

In the most recent work on auxetic rocks, Ji et al. (2019) state that

negative Poisson’s ratio cannot occur in wet volcanic rocks but may appear in a dry basalt with such an extremely high porosity ($\geq 70\%$) that a re-entrant foam structure has formed.

Hence, apart from the laboratory experiments, we expect to detect the negative ν in the seismological studies, in the quartz-rich continental crust with a high geothermal gradient (Ji et al., 2010), quartz-rich and gas-bearing sedimentary rocks, or in dry, highly porous basalts.

Finally, we invoke the examples of auxetic rocks obtained from well-log measurements. Let us consider the work of Castagna and Smith (1994), where the worldwide collection of 25 sets of velocity and density measurements is exhibited. These measurements of brine sands, shales and gas sands, are based on well-log and laboratory data and occur in close in-situ proximity. Based on the velocities of primary and secondary waves, along with the densities, we compute ν . Two samples of gas sands occur to have negative Poisson’s ratio, whereas another sample has a positive value, but very close to zero. Their values are $\nu = -0.18$, $\nu = -0.0162$, and $\nu = 1.02 \times 10^{-4}$, respectively. We find another example of well-log data with negative Poisson’s ratio in Goodway (2001, Table 2). The ostracod shale from the Mannville Group in Western Canadian Sedimentary Basin (WCSB), occurs to be auxetic. The ostracod beds are used in the gas and oil exploration (Hayes et al., 1994), and in particular, oils are sourced from the ostracod shales (Fay et al., 2012). Hence, this is an important case from the explorational point of view. Based on the density, along with the P and S velocities, we again compute Poisson’s ratio and obtain $\nu = -0.11$. Further, Emery and Stewart (2006) present a substantial collection of data from twelve wells in offshore Newfoundland, Eastern Canada. Based on the P and S wave velocities from their Figure 5, we read that subsets of a dataset from at least two wells present $\nu < 0$.

The above real-data examples confirm most of the expectations coming from the laboratory measurements. To conclude, the ideal conditions for a rock to be auxetic are high temperature and low pressure. Additionally, the chances for the auxetic behavior are larger if the rock is dry or gas-bearing, quartz-rich, has numerous cracks, and low porosity.

3.3 Numerical examples

Let us consider some numerical examples to check if the signal that propagates through thin layers would change its shape and magnitude if propagating through the equivalent medium with $\bar{g} \approx 0$. In cases that we examine, Poisson’s ratio of each layer is low. In turn, g ’s of individual constituents are close to zero, which causes the average $\bar{g} \approx 0$. We use some practical examples of ν from Section 3.2.

3.3.1 Wave propagation modelling

In this paper, we analyze the wave propagation in two dimensions, namely, in x_1x_3 -plane. In such a case the elastic equations of motion have the following form.

$$\rho \frac{\partial^2 u_i}{\partial t^2} = \frac{\partial \sigma_{i1}}{\partial x_1} + \frac{\partial \sigma_{i3}}{\partial x_3} + f_i, \quad i \in \{1, 3\}, \quad (58)$$

where ρ is a mass density and f is a body force. To obtain the wave equations, we need to insert—into the equations of motion above—the 2D stress-strain relations and expression (1). To do so, we first reduce relations (4) to two dimensions, namely,

$$\begin{bmatrix} \sigma_{11} \\ \sigma_{33} \\ \sigma_{13} \end{bmatrix} = \begin{bmatrix} C_{11} & C_{13} & 0 \\ C_{13} & C_{33} & 0 \\ 0 & 0 & C_{55} \end{bmatrix} \begin{bmatrix} \varepsilon_{11} \\ \varepsilon_{33} \\ 2\varepsilon_{13} \end{bmatrix}, \quad (59)$$

which are the strain-stress relations valid not only for monoclinic, but also orthogonal, tetragonal, and TI symmetry classes. For cubic case, $C_{33} = C_{11}$, whereas for isotropic class of symmetry, additionally, $C_{13} = C_{11} - 2C_{55}$. (Herein, we do not consider a trigonal class). We solve the resulting elastic wave equations using the open-source seismic modeling code *ewefd2d* in the Madagascar package (Fomel et al., 2013). The code implements a time-domain finite difference method.

To be able to solve the wave equations numerically, we need to define a computational mesh. We model seismic data on a $N_{x_1} \times N_{x_3} = 1500^2$ mesh at uniform $\Delta x_1 = \Delta x_3 = 2$ m spacing. We assume low-frequency stress source injected in x_3 -axis only. For this purpose, we use the Ricker wavelet with a dominant frequency of 12 Hz. We locate the source at $(x_1, x_3) = (1500 \text{ m}, 1500 \text{ m})$ and a receiver at $(x_1, x_3) = (1500 \text{ m}, 1620 \text{ m})$.

In our simulations, we consider a periodic, three-layered system, to which we refer as a PL medium. We propose five different examples of PL media that we denote by roman letters. Media *I–III* represent isotropic layers. Medium *IV* consists of cubic layers, whereas *V* is composed of layers that exhibit either monoclinic, orthotropic, tetragonal or TI symmetry classes. Layers are placed horizontally and uniformly separated by $2\Delta x_3 = 4$ m. Hence, the receiver is separated from the source by a PL medium that consists of ten sets of three layers (in total 120 m). Elasticity coefficients and densities of the layers are presented in Table 3.

	<i>I</i> (iso)	<i>II</i> (iso)	<i>III</i> (iso)	<i>IV</i> (cubic)		<i>V</i> (mon/ort/tetr/TI)	
layer 1	$C_{11} = 37.79$	$C_{11} = 37.79$	$C_{11} = 40$	$C_{11} = 45$	$C_{55} = 10$	$C_{11} = 45$	$C_{55} = 10$
	$C_{55} = 18.89$	$C_{55} = 18.89$	$C_{55} = 20$	$C_{13} = 1.2 \times 10^{-7}$		$C_{13} = 1.2 \times 10^{-7}$	
	$\rho = 2410$	$\rho = 2410$	$\rho = 2410$	$\rho = 2200$		$C_{33} = 35$	$\rho = 2200$
layer 2	$C_{11} = 5.93$	$C_{11} = 20.29$	$C_{11} = 20$	$C_{11} = 20$	$C_{55} = 5$	$C_{11} = 20$	$C_{55} = 5$
	$C_{55} = 2.78$	$C_{55} = 10.14$	$C_{55} = 10$	$C_{13} = 1.0 \times 10^{-7}$		$C_{13} = 1.0 \times 10^{-7}$	
	$\rho = 2100$	$\rho = 2300$	$\rho = 2300$	$\rho = 1800$		$C_{33} = 15$	$\rho = 1800$
layer 3	$C_{11} = 62.44$	$C_{11} = 37.79$	$C_{11} = 40$	$C_{11} = 30$	$C_{55} = 8$	$C_{11} = 30$	$C_{55} = 8$
	$C_{55} = 28.21$	$C_{55} = 18.89$	$C_{55} = 20$	$C_{13} = 0.8 \times 10^{-7}$		$C_{13} = 0.8 \times 10^{-7}$	
	$\rho = 2590$	$\rho = 2410$	$\rho = 2410$	$\rho = 2000$		$C_{33} = 22$	$\rho = 2000$

Table 3: Five different elastic PL media. Elasticity parameters are in GPa, whereas density in kg/m^3 .

Also, using expression (18) and formulas from Appendix A, we compute the elastic coefficients of the media equivalent to *I–V*. The equivalent density is the arithmetic average of densities of individual layers. To model the wave propagation—similarly to the PL case—we insert the computed parameters of the equivalent media into the wave equations.

We compare the displacement propagation in PL and equivalent media by using the following semblance.

$$S = \frac{\sum_i (a_i + b_i)^2}{2 \sum_i (a_i^2 + b_i^2)} \times 100\%, \quad (60)$$

where a_i and b_i are the discrete values of displacement changing with time in both media.

3.3.2 Results

Medium *I* consists of isotropic layers corresponding to gas-bearing sandstones presented in Castagna and Smith (1994) (sets 6, 15, and 12, respectively). Poisson’s ratio of each layer is low, namely, $\nu_1 \approx 2.6 \times 10^{-4}$, $\nu_2 \approx 0.06$, and $\nu_3 \approx 0.10$. As a result, the averaged $\bar{\nu}_2 \approx 0.05$ is low as well. We present the propagation of displacement (x_3 -component) recorded by the receiver in Figure 1a. In

Figure 2, we additionally show the snapshots of wave propagation in both components recorded at time $t = 0.3$ s. We notice that displacements are almost identical for both PL and equivalent media, which is confirmed by $S \approx 99.99\%$. Hence, the product approximation, even if \bar{g} is low, seems to be correct, and the average works properly.

The properties of Medium *II* are similar to gas sandstone from Castagna and Smith (1994) (layer 1 and 3) and ostracod shale from Goodway (2001) (layer 2). In this example, however, we choose the elasticity parameters in such a way that the resulting $\bar{g}_2 \approx 3 \times 10^{-4}$ is very low, but still possible to occur in real data case. The semblance of displacement propagation recorded by the receiver in PL and equivalent medium is high, $S \approx 100\%$. Again, Backus approximation appears to be accurate.

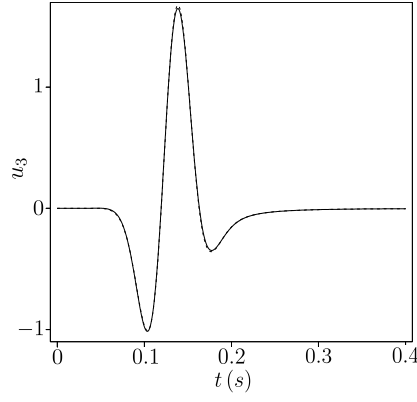
Medium *III* is the idealized version of the previous example. We slightly change the elasticity parameters in a way that \bar{g}_2 is precisely zero, which is probably impossible to achieve in real seismological case. Thus, in this example, the relative error of the product approximation is 100%. Perhaps surprisingly, the aforementioned error does not influence the accuracy of the Backus average, since $S \approx 100\%$.

Previous examples regarded isotropic layers only. From now on, however, we focus on anisotropic constituents. Medium *IV* presents cubic layering. The medium equivalent to cubic layers has a tetragonal symmetry class, as we show in Appendix A. This fact might not be evident for the readers since we have not encountered the above statement or analogical examples in the existing literature. We set C_{13} to have very small values, so that $\bar{g}_2 \approx 3 \times 10^{-9}$ appears to be extremely low. As in previous examples, Backus average works properly ($S \approx 100\%$), which is illustrated by Figures 4 and 5. The last Medium *V* represents layers that can exhibit monoclinic, orthotropic, tetragonal, or TI symmetry class. The product approximation is inaccurate due to $\bar{g}_2 \approx 5 \times 10^{-9}$. However, again it does not affect the Backus approximation that is still accurate since $S \approx 100\%$.

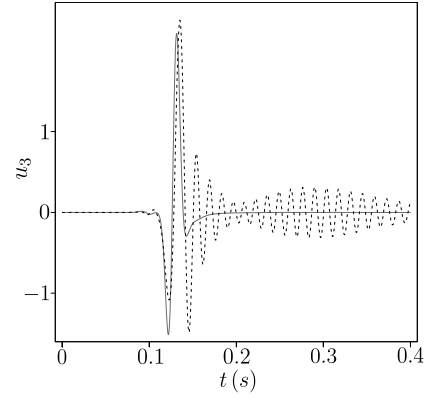
It occurs that the low-frequency assumption seems to raise more concerns than the product assumption. To support the above statement, let us again consider Medium *I*, but exceptionally change the dominant frequency of the Ricker wavelet to 48 Hz; thus, let us increase it four times. Figures 1b and 3 illustrate the inaccuracy of the averaging process confirmed by $S \approx 82.81\%$ only. Later in the text, we refer to this higher-frequency example as to the case I^* . For reference, in Table 4, we present more accurate values of semblances and \bar{g}_2 for all cases I – V .

	<i>I</i>	<i>I</i> [*]	<i>II</i>	<i>III</i>	<i>IV</i>	<i>V</i>
semb.	99.9940	82.8138	99.9996	99.9992	99.9993	99.9988
\bar{g}_2	0.0530	0.0530	3.41×10^{-4}	0	3.44×10^{-9}	4.58×10^{-9}

Table 4: Approximate values of semblances (in %) of signals propagating through thin layers and equivalent media for cases I – V discussed in the main text. The approximate values of averaged \bar{g}_2 are also presented.

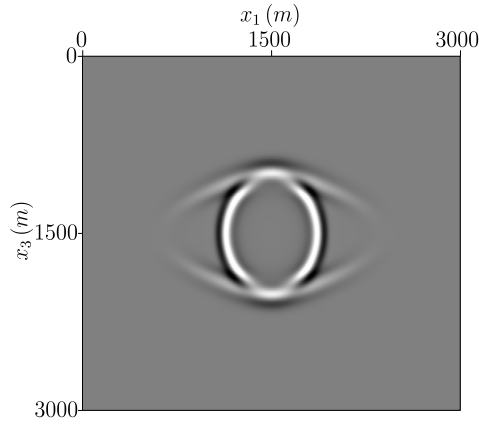


(a) 12 Hz dominant frequency

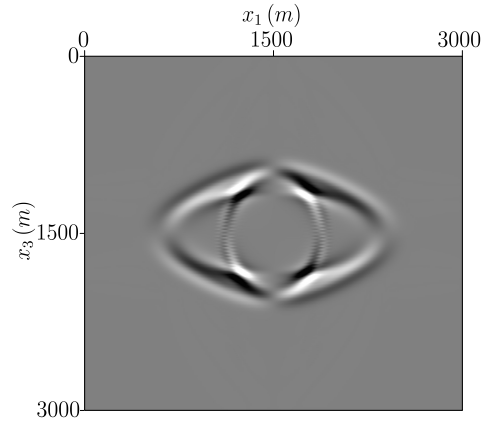


(b) 48 Hz dominant frequency

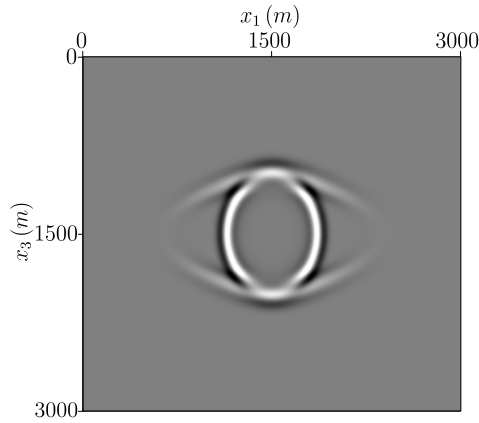
Figure 1: Displacement u_3 recorded by the receiver. Signal in PL and equivalent medium I is denoted by dashed and solid line, respectively.



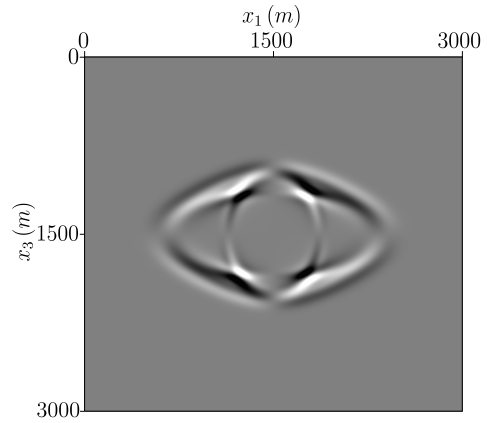
(a) u_3 in PL medium



(b) u_1 in PL medium



(c) u_3 in equivalent medium



(d) u_1 in equivalent medium

Figure 2: Snapshots of displacement u_3 and u_1 in PL and equivalent medium I at time $t = 0.3$ s.

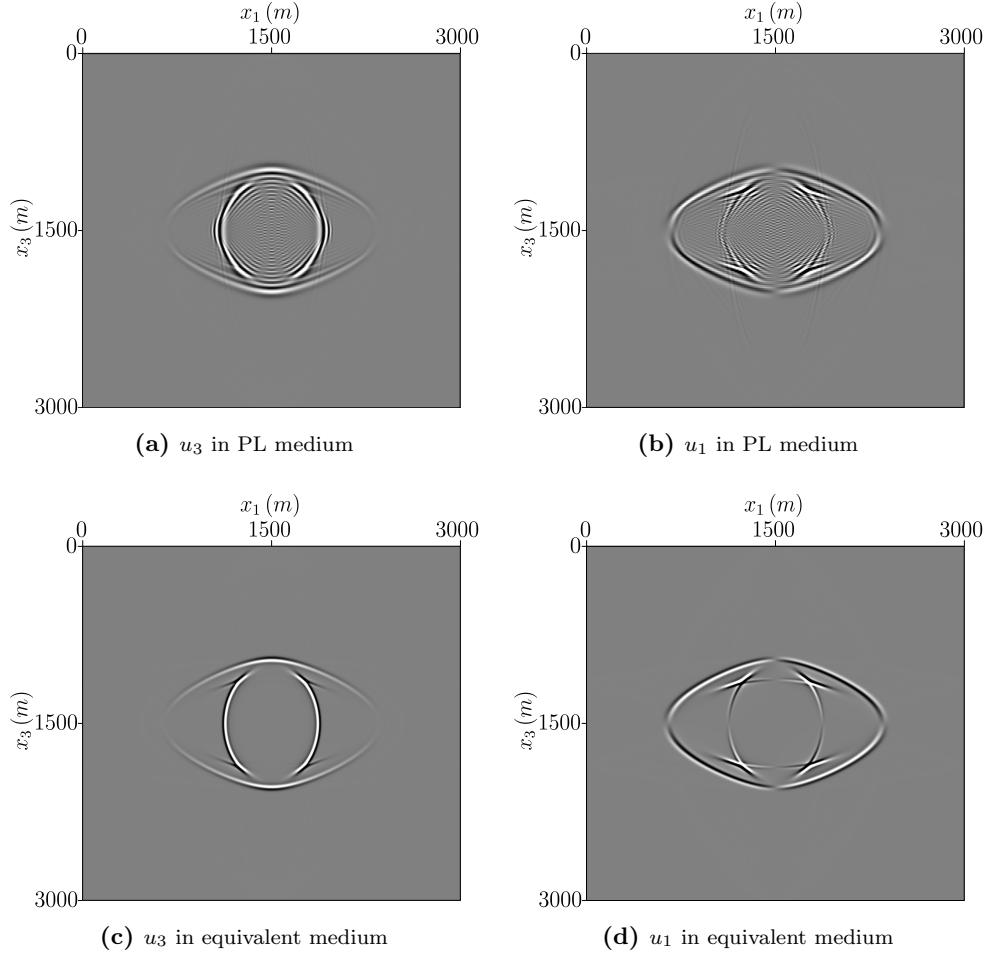


Figure 3: Snapshots of displacement u_3 and u_1 in PL and equivalent medium I^* at time $t = 0.3$ s.

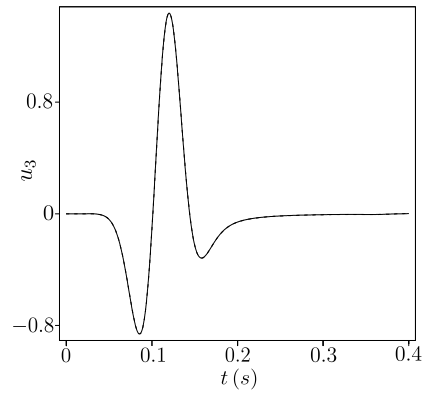


Figure 4: Displacement u_3 recorded by the receiver. Signal in PL and equivalent medium IV is denoted by dashed and solid line, respectively.

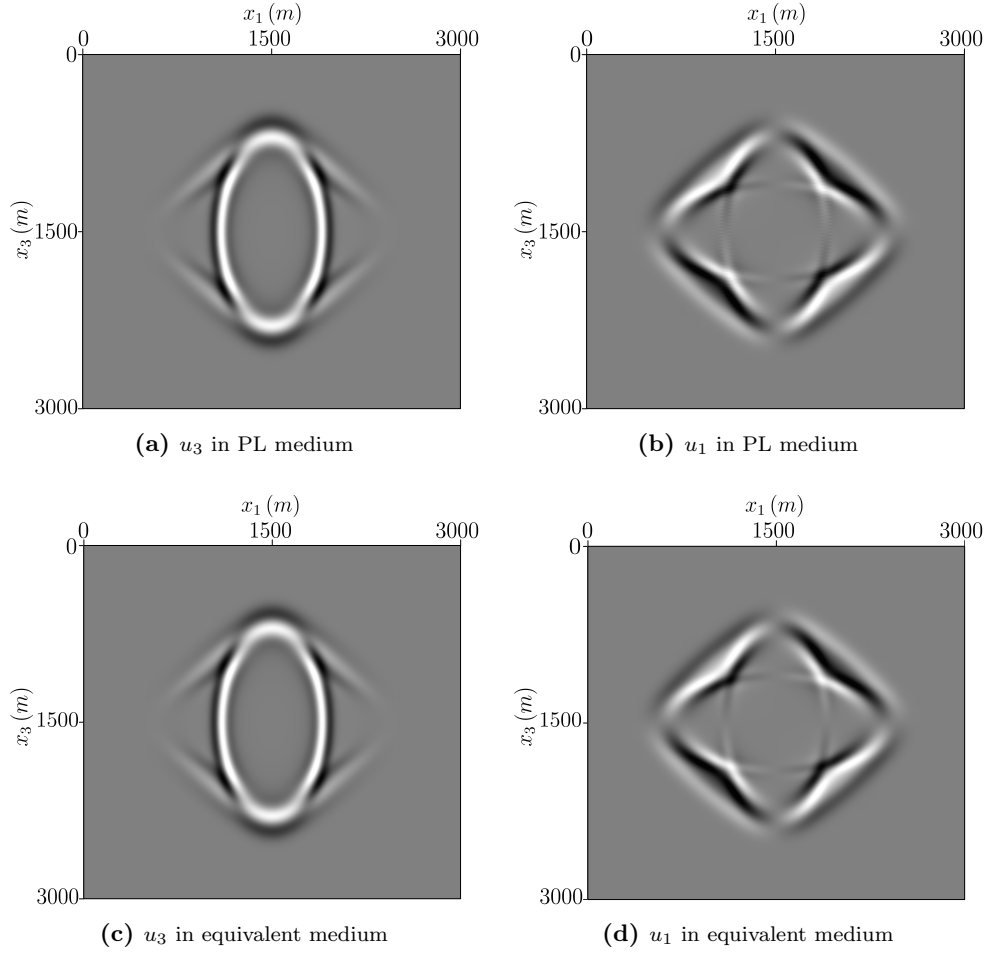


Figure 5: Snapshots of displacement u_3 and u_1 in PL and equivalent medium IV at time $t = 0.3$ s.

4 Conclusions

We focus on the case of product approximation that leads to inaccurate results. We discuss a possibility of its occurrence in physics, in general, and in applied seismology, in particular. We examine numerically the effect of such an inaccuracy on wave propagation in a medium obtained by the Backus average.

In Section 3.1, we present Table 1 that consists of all the possibilities (up to monoclinic class) of rapidly-varying functions g . Table 2 indicates which g may be negative and still obey the stability conditions. In turn, negative g (or positive, but low values of g) in certain layers may lead to the average $\bar{g} \approx 0$, which makes the product approximation inaccurate. As discussed in Section 3.2, for isotropic, cubic, TI, and tetragonal symmetry classes, negative g is tantamount to negative Poisson’s ratio in some direction. Based on the literature review, we show that there are numerous examples in which $\nu < 0$ occurs in practice. Thus, the problematic case of product approximation is likely to occur in real seismological cases, not as thought previously (Bos et al., 2018). In general, the chances for negative, or low positive Poisson’s ratio are larger if the rock is dry or gas-bearing, is quartz-rich, has numerous cracks and low porosity, occurs in a high-temperature or low-pressure environment.

In Section 3.3, we perform several 2D numerical simulations of wave propagation in layered and equivalent media with $\bar{g} \approx 0$. Based on these examples, we conclude that the problematic case of product approximation that causes the Backus average to be inaccurate does not affect the wave propagation in a meaningful manner. The product assumption occurs to be much less critical than the long-wave and thin layers assumption.

Please note that our numerical analysis is not entirely complete. We neither consider 3D examples, nor the cases of layers exhibiting generally-anisotropic or trigonal symmetry classes. However, given our simulations, we expect that the influence of $\bar{g} \approx 0$ on the wave propagation in equivalent medium obtained by the Backus average should also be marginal in these, low-symmetry or 3D examples.

Acknowledgements

We wish to thank Michael A. Slawinski and David Dalton for their comments. The author has no conflict of interests to declare.

References

- Backus, G. E. (1962). Long-wave elastic anisotropy produced by horizontal layering. *J. Geophys. Res.*, 67(11):4427–4440.
- Bakulin, A. and Grechka, V. (2003). Effective anisotropy of layered media. *Geophysics*, 68(6):1817–1821.
- Baughman, R. H., Stafstrom, S., Cui, C., and Dantas, S. O. (1998). Materials with Negative Compressibilities in One or More Dimensions. *Science*, 279(5356):1522–1524.
- Beljankin, D. S. and Petrov, V. P. (1938). Occurrence of cristobalite in a sedimentary rock. *Am. Mineral.*, 23(3):153–155.
- Bos, L., Dalton, D. R., Slawinski, M. A., and Stanoev, T. (2017). On Backus Average for Generally Anisotropic Layers. *J. Elast.*, 127(2):179–196.
- Bos, L., Danek, T., Slawinski, M. A., and Stanoev, T. (2018). Statistical and numerical Considerations of Backus-Average Product Approximation. *J. Elast.*, 132(1):141–159.

- Calvert, S. E., Burns, R. G., Smith, J. V., and Kempe, D. R. C. (1977). Mineralogy of Silica Phases in Deep-Sea Cherts and Porcelanites [and Discussion]. *Phil. Trans. Roy. Soc. Lond. Math. Phys. Sci.*, 286(1336):239–252.
- Carcione, J. M., Kosloff, D., and Behle, A. (1991). Long-wave anisotropy in stratified media: A numerical test. *Geophysics*, 56(2):245–254.
- Castagna, J. P. and Smith, S. W. (1994). Comparison of AVO indicators: A modeling study. *Geophysics*, 59(12):1849–1855.
- Coyner, K. B. (1984). *Effects of stress, pore pressure, and pore fluids on bulk strain, velocity, and permeability in rocks*. PhD thesis, Massachusetts Institute of Technology.
- Damby, D. E., Llewellyn, E. W., Horwell, C. J., Williamson, B. J., Najorka, J., Cressey, G., and Carpenter, M. (2014). The α – β phase transition in volcanic cristobalite. *J. Appl. Crystallogr.*, 47(4):1205–1215.
- Dvorkin, J., Moos, D., Packwood, J. L., and Nur, A. M. (1999). Identifying patchy saturation from well logs. *Geophysics*, 64(6):1756–1759.
- Dziwonoński, A. M. and Anderson, D. L. (1981). Preliminary reference Earth model. *Phys. Earth Planet. Inter.*, 25(4):297–356.
- Emery, D. J. and Stewart, R. R. (2006). Using VP/VS to explore for sandstone reservoirs: well log and synthetic seismograms from the Jeanne d’Arc basin, offshore Newfoundland. *CREWES Research Report*, 18(1):1–20.
- Fay, M., Larter, S., Bennett, B., Snowden, L., and Fowler, M. (2012). Petroleum Systems and Quantitative Oil Chemometric Models for Heavy Oils in Alberta and Saskatchewan to Characterize Oil-Source Correlations. *GeoConvention 2012:Vision*.
- Fomel, S., Sava, P., Vlad, I., Liu, Y., and Bashkardin, V. (2013). Madagascar: Open-source software project for multidimensional data analysis and reproducible computational experiments. *J. Open Res. Softw.*, 1(1):e8.
- Freund, D. (1992). Ultrasonic compressional and shear velocities in dry clastic rocks as a function of porosity, clay content, and confining pressure. *Geophys. J. Int.*, 108(1):125–135.
- Goodway, B. (2001). AVO and Lamé constants for rock parameterization and fluid detection. *CSEG Recorder*, 26(6):39–60.
- Gregory, A. R. (1976). Fluid saturation effect on dynamic elastic properties of sedimentary rocks. *Geophysics*, 41(5):895–921.
- Grima, J. N., Gatt, R., Zammit, V., Williams, J. J., Evans, K. E., Alderson, A., and Walton, R. I. (2007). Natrolite: a zeolite with negative Poisson’s ratios. *J. Appl. Phys.*, 101(8):086102.
- Grima, J. N., Jackson, R., Alderson, A., and Evans, K. E. (2000). Do Zeolites Have Negative Poisson’s Ratios? *Advanced Materials*, 12(24):1912–1918.
- Han, D.-H. (1986). *Effects of porosity and clay content on acoustic properties of sandstones and unconsolidated sediments*. PhD thesis, Stanford University.
- Hay, R. L. (1986). Geologic Occurrence of Zeolites and Some Associated Minerals. *Stud. Surf. Sci. Catal.*, 28(1):35–40.
- Hayes, B. J. R., Christopher, J. R., Rosenthal, L., Los, G., McKercher, B., Minken, D., Tremblay, Y. M., and Fennel, J. (1994). Cretaceous Mannville Group of the Western Canada Sedimentary Basin; in Geological Atlas of the Western Canada Sedimentary

- Basin. *Canadian Society of Petroleum Geologists and Alberta Research Council*, 19(URL: <https://ags.aer.ca/publications/chapter-19-cretaceous-mannville-group.htm>).
- Helbig, K. (1984). Anisotropy and dispersion in periodically layered media. *Geophysics*, 49(4):364–373.
- Helbig, K. (1994). *Foundations of anisotropy for exploration seismics*. Pergamon Press, 1st edition.
- Hommand-Etienne, F. and Houpert, R. (1989). Thermally Induced Microcracking in Granites: Characterization and Analysis. *Int. J. Rock Mech. Min. Sci. Geomech. Abstr.*, 26(2):125–134.
- Ji, S., Li, L., Motra, H. B., Wuttke, F., Sun, S., Michibayashi, K., and Salisbury, M. H. (2018). Poisson’s Ratio and Auxetic Properties of Natural Rocks. *J. Geophys. Res. Solid Earth*, 123(2):1161–1185.
- Ji, S., Sun, S., Wang, Q., and Marcotte, D. (2010). Lamé parameters of common rocks in the earth’s crust and upper mantle. *J. Geophys. Res. Solid Earth*, 115(B6).
- Ji, S., Wang, Q., and Li, L. (2019). Seismic velocities, Poisson’s ratios and potential auxetic behavior of volcanic rocks. *Tectonophysics*, 766(1):270–282.
- Jizba, D. (1991). *Mechanical and acoustical properties of sandstones and shales*. PhD thesis, Stanford University.
- Kudela, I. and Stanoev, T. (2018). On possible issues of Backus average. *arXiv:1804.01917 [physics.geo-ph]*.
- Lakes, R. S. (2017). Negative-Poisson’s-Ratio Materials: Auxetic Solids. *Annu. Rev. Mater. Res.*, 47(1):63–81.
- Liner, C. and Fei, T. (2007). The backus number. *Lead. Edge*, 26(4):420–426.
- Mavko, G. and Jizba, D. (1994). The relation between seismic P- and S-wave velocity dispersion in saturated rocks. *Geophysics*, 59(1):87–92.
- Mavko, G., Mukerji, T., and Dvorkin, J. (2009). *The rock physics handbook*. Cambridge, 2nd edition.
- McKnight, R. E. A., Moxon, T., Buckley, A., Taylor, P. A., Darling, T. W., and Carpenter, M. A. (2008). Grain size dependence of elastic anomalies accompanying the α - β phase transition in polycrystalline quartz. *J. Phys. Condens. Matter*, 20(7):075229.
- Mizota, C., Toh, N., and Matsuhisa, Y. (1987). Origin of cristobalite in soils derived from volcanic ash in temperate and tropical regions. *Geoderma*, 39(4):323–330.
- Mouchat, F. and Coudert, F. X. (2014). Necessary and Sufficient Elastic Stability Conditions in Various Crystal Systems. *Phys. Rev. B*, 90(22):1–4.
- Nur, A. and Simmons, G. (1969). The effect of saturation on velocity in low porosity rocks. *Earth Planet. Sci. Lett.*, 7(2):183–193.
- Sanchez-Valle, C., Lethbridge, Z. A. D., Sinogeikin, S. V., Williams, J. J., Walton, R. I., Evans, K. E., and Bass, J. D. (2008). Negative Poisson’s ratios in siliceous zeolite MFI-silicalite. *J. Chem. Phys.*, 128(18):184503.
- Schoenberg, M. and Muir, F. (1989). A calculus for finely layered anisotropic media. *Geophysics*, 54(5):581–589.
- Slawinski, M. A. (2015). *Waves and rays in elastic continua*. World Scientific, 3rd edition.
- Slawinski, M. A. (2018). *Waves and rays in seismology: Answers to unasked questions*. World Scientific, 2nd edition.

Yeganeh-Haeri, A., Weidner, D. J., and Parise, J. B. (1992). Elasticity of α -Cristobalite: A Silicon Dioxide with a Negative Poisson's Ratio. *Science*, 257(5070):650–652.

Zaitsev, V. Y., Radostin, A. V., Pasternak, E., and Dyskin, A. (2017). Extracting real-crack properties from non-linear elastic behaviour of rocks: abundance of cracks with dominating normal compliance and rocks with negative Poisson ratios. *Nonlinear Process. Geophys.*, 24(3):543–551.

A Backus average for anisotropic layers

Let us write the strain-stress relations in two dimensions (x_1x_3 -plane), namely,

$$\sigma_{11} = C_{11}\varepsilon_{11} + C_{13}\varepsilon_{33}, \quad (61)$$

$$\sigma_{33} = C_{13}\varepsilon_{11} + C_{33}\varepsilon_{33}, \quad (62)$$

$$\sigma_{13} = 2C_{55}\varepsilon_{13}, \quad (63)$$

which are the relations valid for the monoclinic, orthotropic, tetragonal, and TI symmetry class. Upon a rearrangement, we get

$$\sigma_{11} = \left(C_{11} - \frac{C_{13}^2}{C_{33}}\right)\varepsilon_{11} + \left(\frac{C_{13}}{C_{33}}\right)\sigma_{33}, \quad (64)$$

$$\varepsilon_{33} = -\left(\frac{C_{13}}{C_{33}}\right)\varepsilon_{11} + \left(\frac{1}{C_{33}}\right)\sigma_{33}, \quad (65)$$

$$\frac{\partial u_1}{\partial x_3} = \left(\frac{1}{C_{55}}\right)\sigma_{13} - \frac{\partial u_3}{\partial x_1}. \quad (66)$$

Let us treat the above equations as the stress-strain relations that correspond to many individual constituents that we want to average. To perform the averaging process, we use the three following properties: the average of the sum is a sum of the average, the average of the derivative is a derivative of the average, and, finally, the product approximation. We obtain

$$\overline{\sigma_{11}} = \left[\overline{\left(C_{11} - \frac{C_{13}^2}{C_{33}}\right)} + \overline{\left(\frac{C_{13}}{C_{33}}\right)}^2 \overline{\left(\frac{1}{C_{33}}\right)}^{-1}\right] \overline{\varepsilon_{11}} + \overline{\left(\frac{C_{13}}{C_{33}}\right)} \overline{\left(\frac{1}{C_{33}}\right)}^{-1} \overline{\sigma_{33}}, \quad (67)$$

$$\overline{\sigma_{33}} = \overline{\left(\frac{C_{13}}{C_{33}}\right)} \overline{\left(\frac{1}{C_{33}}\right)}^{-1} \overline{\varepsilon_{11}} + \overline{\left(\frac{1}{C_{33}}\right)}^{-1} \overline{\sigma_{33}}, \quad (68)$$

$$\overline{\sigma_{13}} = \overline{\left(\frac{1}{C_{55}}\right)}^{-1} 2 \overline{\varepsilon_{13}}. \quad (69)$$

Comparing equations (67)–(69) with equations (61)–(63), we see that the equivalent elasticity parameters are equal to

$$C_{11}^{\text{eq}} = \overline{\left(C_{11} - \frac{C_{13}^2}{C_{33}}\right)} + \overline{\left(\frac{C_{13}}{C_{33}}\right)}^2 \overline{\left(\frac{1}{C_{33}}\right)}^{-1}, \quad (70)$$

$$C_{13}^{\text{eq}} = \overline{\left(\frac{C_{13}}{C_{33}}\right)} \overline{\left(\frac{1}{C_{33}}\right)}^{-1}, \quad (71)$$

$$C_{33}^{\text{eq}} = \left(\frac{1}{C_{33}} \right)^{-1}, \quad (72)$$

$$C_{55}^{\text{eq}} = \left(\frac{1}{C_{55}} \right)^{-1}, \quad (73)$$

and the resulting medium is either monoclinic, orthotropic, tetragonal, or TI. If layers have cubic symmetry, then $C_{33} = C_{11}$. In such a case, $C_{33}^{\text{eq}} \neq C_{11}^{\text{eq}}$, which means that the equivalent medium is not cubic. To understand what is the symmetry class of the medium equivalent to cubic layers, we need to derive the analogous equivalent parameters, but for 3D case. Upon an analogous procedure, shown above, we get

$$C_{11}^{\text{eq}} = \overline{\left(C_{11} - \frac{C_{13}^2}{C_{11}} \right)} + \overline{\left(\frac{C_{13}}{C_{11}} \right)^2 \left(\frac{1}{C_{11}} \right)^{-1}}, \quad (74)$$

$$C_{12}^{\text{eq}} = \overline{\left(C_{13} - \frac{C_{13}^2}{C_{11}} \right)} + \overline{\left(\frac{C_{13}}{C_{11}} \right)^2 \left(\frac{1}{C_{11}} \right)^{-1}}, \quad (75)$$

$$C_{13}^{\text{eq}} = \overline{\left(\frac{C_{13}}{C_{11}} \right) \left(\frac{1}{C_{11}} \right)^{-1}}, \quad (76)$$

$$C_{33}^{\text{eq}} = \left(\frac{1}{C_{11}} \right)^{-1}, \quad (77)$$

$$C_{55}^{\text{eq}} = \left(\frac{1}{C_{55}} \right)^{-1}, \quad (78)$$

$$C_{66}^{\text{eq}} = \overline{C_{55}}, \quad (79)$$

where $C_{11}^{\text{eq}} = C_{22}^{\text{eq}}$, $C_{13}^{\text{eq}} = C_{23}^{\text{eq}}$, and $C_{55}^{\text{eq}} = C_{44}^{\text{eq}}$. The equivalent medium has six independent elasticity parameters and exhibits the tetragonal symmetry class.

B Backus procedure for a trigonal tensor

First, we write the stress-strain relations in a trigonal medium (expressed in a natural coordinate system) as

$$\sigma_{11} = C_{11}\varepsilon_{11} + C_{12}\varepsilon_{22} + C_{13}\varepsilon_{33} + C_{15}\frac{\partial u_1}{\partial x_3} + C_{15}\frac{\partial u_3}{\partial x_1}, \quad (80)$$

$$\sigma_{22} = C_{12}\varepsilon_{11} + C_{11}\varepsilon_{22} + C_{13}\varepsilon_{33} - C_{15}\frac{\partial u_1}{\partial x_3} - C_{15}\frac{\partial u_3}{\partial x_1}, \quad (81)$$

$$\sigma_{33} = C_{13}\varepsilon_{11} + C_{13}\varepsilon_{22} + C_{33}\varepsilon_{33}, \quad (82)$$

$$\sigma_{23} = C_{44}\frac{\partial u_2}{\partial x_3} + C_{44}\frac{\partial u_3}{\partial x_2} - 2C_{15}\varepsilon_{12}, \quad (83)$$

$$\sigma_{13} = C_{44}\frac{\partial u_1}{\partial x_3} + C_{44}\frac{\partial u_3}{\partial x_1} + C_{15}\varepsilon_{11} - C_{15}\varepsilon_{22}, \quad (84)$$

$$\sigma_{12} = (C_{11} - C_{12})\varepsilon_{12} - C_{15}\frac{\partial u_2}{\partial x_3} - C_{15}\frac{\partial u_3}{\partial x_2}. \quad (85)$$

We can directly rewrite equations (82)–(84) in a manner that the nearly-constant stresses and strains are on the right-hand side, whereas the sole varying function of displacements is on the left-hand side. We get,

$$\varepsilon_{33} = \underbrace{\sigma_{33} \left(\frac{1}{C_{33}} \right)}_{g_1} - \underbrace{\left(\frac{C_{13}}{C_{33}} \right)}_{g_2} \varepsilon_{11} - \underbrace{\left(\frac{C_{13}}{C_{33}} \right)}_{g_3} \varepsilon_{22}, \quad (86)$$

$$\frac{\partial u_2}{\partial x_3} = \sigma_{23} \underbrace{\left(\frac{1}{C_{44}} \right)}_{g_4} - \frac{\partial u_3}{\partial x_2} - \underbrace{\left(\frac{C_{15}}{C_{44}} \right)}_{g_t} 2\varepsilon_{12}, \quad (87)$$

$$\frac{\partial u_1}{\partial x_3} = \sigma_{13} \underbrace{\left(\frac{1}{C_{44}} \right)}_{g_5} - \frac{\partial u_3}{\partial x_1} - \left(\frac{C_{15}}{C_{44}} \right) \varepsilon_{11} + \left(\frac{C_{15}}{C_{44}} \right) \varepsilon_{22}. \quad (88)$$

Now, we insert the right-hand side of equation (86) and (88) into equations (80) and (81). Also, we insert the right-hand side of (87) into (85). Upon simple calculations, we obtain

$$\sigma_{11} = \sigma_{33} \left(\frac{C_{13}}{C_{33}} \right) + \sigma_{13} \left(\frac{C_{15}}{C_{44}} \right) + \underbrace{\left(C_{11} - \frac{C_{13}^2}{C_{33}} - \frac{C_{15}^2}{C_{44}} \right)}_{g_6} \varepsilon_{11} + \underbrace{\left(C_{12} - \frac{C_{13}^2}{C_{33}} + \frac{C_{15}^2}{C_{44}} \right)}_{g_7} \varepsilon_{22}, \quad (89)$$

$$\sigma_{22} = \sigma_{33} \left(\frac{C_{13}}{C_{33}} \right) - \sigma_{13} \left(\frac{C_{15}}{C_{44}} \right) + \left(C_{12} - \frac{C_{13}^2}{C_{33}} + \frac{C_{15}^2}{C_{44}} \right) \varepsilon_{11} + \underbrace{\left(C_{11} - \frac{C_{13}^2}{C_{33}} - \frac{C_{15}^2}{C_{44}} \right)}_{g_8} \varepsilon_{22}, \quad (90)$$

$$\sigma_{12} = -\sigma_{23} \left(\frac{C_{15}}{C_{44}} \right) - \underbrace{\left(\frac{C_{11} - C_{12}}{2} - \frac{C_{15}^2}{C_{44}} \right)}_{g_9} 2\varepsilon_{12}. \quad (91)$$

Terms in parenthesis in equations (86)–(91) correspond to various g ; we denote them as g_i or g_t . We notice that in case of trigonal symmetry, $g_2 = g_3$, $g_4 = g_5$, and $g_6 = g_8$.

C Relation between n_1 , n_2 , g_2^{ort} , and g_3^{ort}

Lemma C.1. *If numerators of Poisson's ratios $n_1 > 0$ and $n_2 > 0$, then the stability conditions for orthotropic media do not allow $g_2^{\text{ort}} < 0$ and $g_3^{\text{ort}} < 0$.*

Proof. Consider $n_1 > 0$, namely,

$$C_{13}C_{22} - C_{12}C_{23} > 0. \quad (92)$$

Let us assume that $g_2^{\text{ort}} < 0$ and $g_3^{\text{ort}} < 0$. Since, according to stability conditions, $C_{33} \geq 0$, the above assumption is tantamount to $C_{13} < 0$ and $C_{23} < 0$. We also know that $C_{22} \geq 0$, thus, to satisfy expression (94) C_{12} must be positive. Therefore, we can write

$$\frac{C_{13}C_{22}}{C_{12}} > C_{23}. \quad (93)$$

Consider $n_2 > 0$, namely,

$$C_{23}C_{11} > C_{12}C_{13}. \quad (94)$$

Both sides are negative, where C_{11} and C_{12} must be positive. This inequality allows us to insert some larger value in the place of C_{23} . If we insert the left-hand side of inequality (97), we get

$$\frac{C_{13}C_{11}C_{22}}{C_{12}} > C_{12}C_{13}. \quad (95)$$

Since C_{13} is assumed to be negative and C_{12} must be negative, we obtain

$$C_{11}C_{22} < C_{12}^2, \quad (96)$$

which is not allowed by the stability condition. \square

Lemma C.2. *If numerators of Poisson's ratios $n_1 < 0$ and $n_2 < 0$, then the stability conditions for orthotropic media do not allow $g_2^{\text{ort}} > 0$ and $g_3^{\text{ort}} > 0$.*

Proof. Consider $n_1 < 0$, we get

$$\frac{C_{12}C_{23}}{C_{22}} > C_{13}. \quad (97)$$

Also, consider $n_2 < 0$, namely,

$$C_{12}C_{13} > C_{23}C_{11}. \quad (98)$$

Let us assume that $g_2^{\text{ort}} > 0$ and $g_3^{\text{ort}} > 0$. In such a case, both sides of inequalities (97) and (98) are positive. We can insert greater value than C_{13} in the inequality (98). We obtain,

$$\frac{C_{12}^2C_{23}}{C_{22}} > C_{23}C_{11}. \quad (99)$$

Since, $C_{23} > 0$ we obtain

$$C_{12}^2 > C_{11}C_{22}, \quad (100)$$

which is not allowed by the stability condition. \square

Similar strategy can be used to prove that if $n_1 < 0$ and $n_2 > 0$ then $g_2^{\text{ort}} > 0$ and $g_3^{\text{ort}} < 0$ are not allowed, or, conversely, if $n_1 > 0$ and $n_2 < 0$ then $g_2^{\text{ort}} < 0$ and $g_3^{\text{ort}} > 0$ are not allowed.